Multiscale Modeling of Radical and Vibrational Pathways in Plasma-Assisted Ammonia Synthesis on Fe(110) and Ni(111)

Oluwatosin A. Ohiro*, Samuel A. Ogunwale, Bryan R. Goldsmith
Department of Chemical Engineering, University of Michigan, Ann Arbor, MI, 48104, USA

MICHIGAN ENGINEERING
UNIVERSITY OF MICHIGAN

Goldsmith Lab: Materials, Modeling, Data Science, Descriptors, Catalysis

Background and Motivation

- The Haber–Bosch process for ammonia ($NH_{3(g)}$) synthesis is responsible for 1–2% of global energy consumption[1]

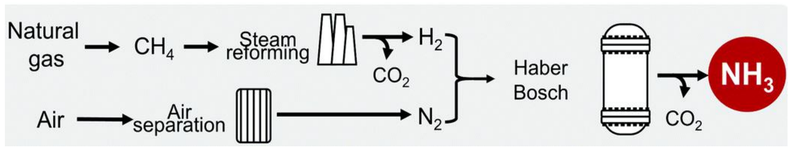

New catalytic technology is needed for sustainable ammonia synthesis

- Low temperature plasma (LTP) assisted catalysis is a potential complement to traditional thermocatalytic chemical conversion processes, such as $NH_{3(g)}$ synthesis.[2]
- Activate difficult molecules (e.g., N_2) and enhance reactivity at low temperature

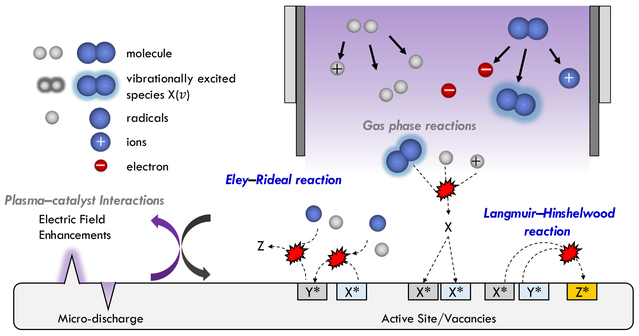

- Complex interactions affect elucidation of the mechanism for LTP-assisted $NH_{3(g)}$ synthesis[1]
- Understanding interactions in LTP system allows for optimization of reaction conditions, catalyst type, and energy/environmental considerations

Uncertainty in Species Activity for $NH_{3(g)}$ Synthesis

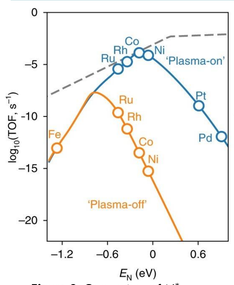

Figure 2. Comparison of $N^*_{2,v}$ distribution-weighted (plasma-on) and thermal (plasma-off) $NH_{3(g)}$.[3]

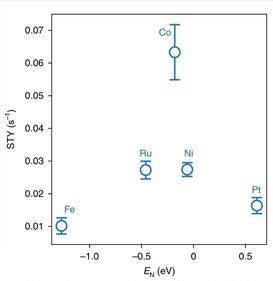

Figure 3. Measured $NH_{3(g)}$ STYs in the DBD reactor on metal/Al_2O_3 catalysts as a function of the DFT-calculated nitrogen adsorption energy. T = 438 K.[3]

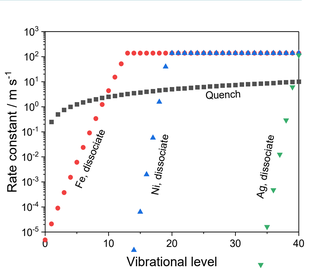

Figure 4. Upper bounds on the ratio of rates of dissociative adsorption to the rates of $N_{2(v)}$ over Fe, Ni, and Ag metal wool catalysts as a function of vibrational level at the experimental surface temperature

- Initial computational results show orders of magnitude differences in $NH_{3(g)}$ production when only $N_{2(g),v}$ are consider only. High vibrational levels with lower dissociation barriers lead to higher reaction rate for $NH_{3(g)}$
- The identity of most active metal for $NH_{3(g)}$ synthesis changes from prior computational analysis
- Experimental results show similar orders of magnitude of $NH_{3(g)}$ production across metals
- Rate constant analysis reveals that highly vibrationally excited $N_{2(g),v}$ may not be active during the reaction due to surface quenching reactions

Goal: Elucidate how various LTP-generated species yield similar NH_3 rates across different metal catalyst

Modeling Methodology

- We study plasma species generated in RF reactor interactions in a packed bed reactor (PBR)
- We compare 5 microkinetic models increasing complexity to elucidate how different species affect the rate of NH_3 formation and examine which model rationalizes our experiments on Fe and Ni catalysts

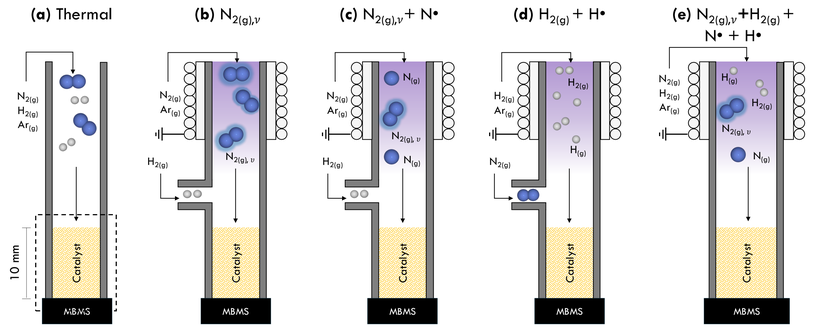

Model parameters are computed via density functional theory (DFT) and mean-field microkinetic models are constructed to compare to experiments results.

DFT

Many-body problem → Electronic energy, Free Energy

Microkinetic modelling

Experiment Reaction Conditions (T,P)

Model Comparison with Experiment

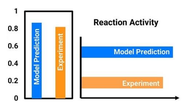

1 Reactions

$$N_{2,v} + * \rightleftharpoons N^*_{2,v}$$
$$N^*_{2(v)} + * \rightleftharpoons 2N^*$$
$$H_2 + 2^* \rightleftharpoons 2H^*$$
$$N^* + H^* \rightleftharpoons NH^*$$

2 From thermodynamics

Equilibrium rate constant are obtained from each chemical reaction

$$K_{equil} = \frac{k_B T}{h} e^{\frac{\Delta E_{rxn} - T\Delta S}{RT}}$$

3 Forward rate constants

- *Langmuir Hinshelwood reactions*

$$k_f = \frac{k_B T}{h} e^{\frac{\Delta S^\ddagger}{R}} e^{\frac{\Delta E^\ddagger}{RT}}$$

… for $N_{2(g),\,v}$ dissociation

$$k_f = \frac{k_B T}{h} e^{\frac{\Delta S^\ddagger}{R}} e^{\frac{\Delta E^\ddagger - \alpha E_{vib}}{RT}}$$

- *Eley-Rideal Reactions*

$$k_f = \frac{k_B T}{h} e^{\frac{\Delta S^\ddagger}{R}}$$

4 Backward rate constants

$$k_r = k_f / K_{equil}$$

5 Reaction Rate

$$r_j = k_{j,f} \prod_i C_i^{\nu^f_{i,j}} - k_{j,r} \prod_i C_i^{\nu^r_{i,j}}$$

6 Transient flow behavior in a PBR

$$\frac{\partial C_i}{\partial t} = -\nu \frac{\partial C_i}{\partial V} + \sum_j^n r_j$$

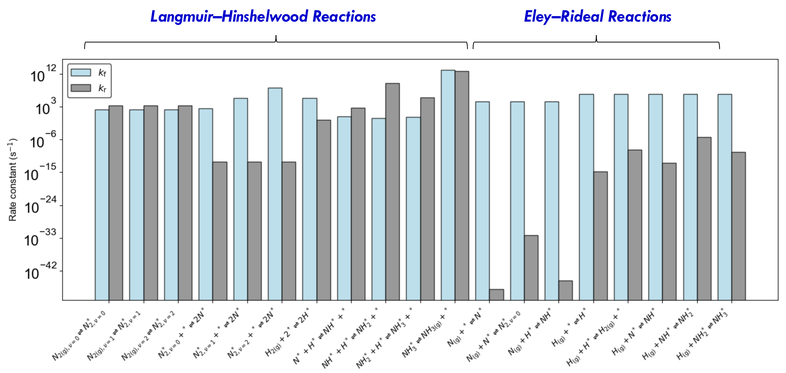

Figure 5. Reaction rate kinetics involving LTP generated species interaction with surface metal catalyst on Fe (110) at 517 K and 1 bar. Blue bars represents the forward rate constants, while the gray bars represents the reverse reaction rates.

Reaction Mechanism Elucidation Results

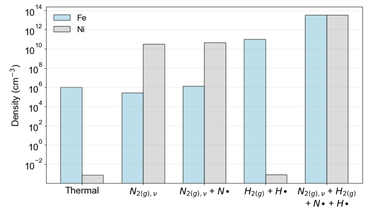

Figure 6. $NH_{3(g)}$ densities at the outlet of the PBR reactor on on Fe(110) and Ni (111) metal surface. Operating conditions: 1 conditions: 1 atm, 517 K, 1 SLM total flow rate. Feed gas composition: 0.5% $N_{2(g)}$, 2.5% $H_{2(g)}$, 97 % $Ar_{(g)}$. LTP species are species are generated in the upstream RF plasma reactor before before entering the PBR. N• densities = 1×10^{14} cm^{-3}, H• densities = 1×10^{16} cm^{-3}.

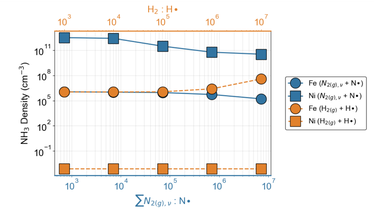

Figure 7. $NH_{3(g)}$ densities at the outlet of the PBR reactor on Fe(110) and Ni (111) metal surface at various LTP RF power for Model $N_{2(g),v}$+ N• and Model $H_{2(g)}$ + H•. Operating conditions: 1 atm, 517 K, 1 SLM total flow rate. Feed gas composition: 0.5% $N_{2(g)}$, 2.5% $H_{2(g)}$, 97 % $Ar_{(g)}$.

- Fe shows better performance compared to Ni as expected under pure thermal catalysis
- Ni performance improves due to easier nitrogen fixation on the catalyst surface from $N_{2(g),v}$
- Fe turnover rate is improved in the presence of H radicals, indicating that thermal $NH_{3(g)}$ production is limited due to the absence of H radicals.
- We achieve parity in metal performance when all limiting reactants are indued in the model
- A synergistic effect is seen in overall $NH_{3(g)}$ density when all LTP-generated species are included in the model (i.e. $N_{2(g),v}$+$H_{2(g)}$ + N• + H•)

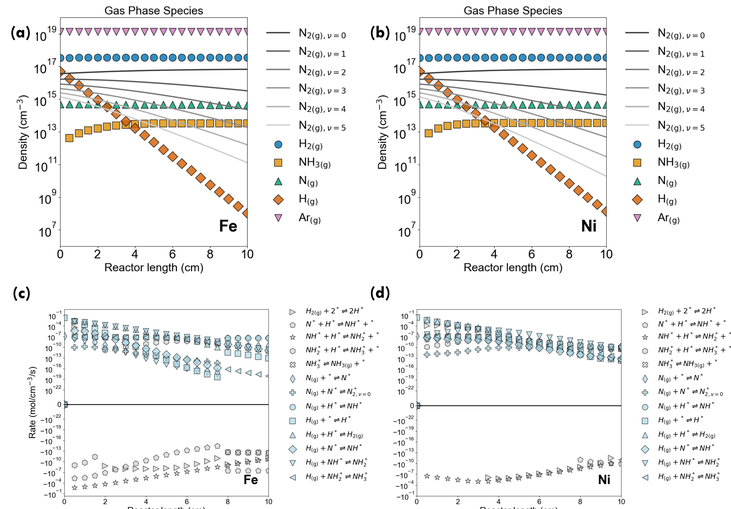

Figure 8. **(a, b)** Gas densities along the length of the PBR on **(a)** Fe and **(b)** Ni catalyst. Vibrationally excited $N_{2(g),v}$ are shown in grayscale, only the first six vibrational levels are shown for visual clarity. **(c, d)** Elementary reaction rates along the reactor. Langmuir Hensel wood reactions are in grey, E-R reations are in blue on **(c)** Fe and **(d)** Ni. Operating conditions: 1 atm, 517 K, 1 SLM total flow rate. Feed gas composition: 0.5% $N_{2(g)}$, 2.5% $H_{2(g)}$, 97 % $Ar_{(g)}$. LTP species are generated in the upstream RF plasma reactor before entering the catalytic bed. N• densities = 1×10^{14} cm^{-3}, H• densities = 1×10^{16} cm^{-3}.

- Faster Eley–Rideal kinetics dominate reaction pathway for $NH_{3(g)}$ production
- H• are consumed at a much faster rate than N• densities. When present, H• become the dominant source of hydrogenation.
- Increase in $N_{2(g),v=0}$ at reactor outlet is due to quenching reaction of higher excited states and recombination of N•

Conclusions

- Increasing model complexity to include Eley-Rideal reactions reconciles the discrepancy between experimental and computational results for Fe and Ni catalysts.
- Similar analyses should be conducted across other transition metals to determine whether these trends persist more generally.

References

[1] Sun, J.; Alam, D.; Daiyan, R.; Masood, H.; Zhang, T.; Zhou, R.; J. Cullen, P.; C. Lovell, E.; Ali Jalili; Amal, R. Energy Environ. Sci. 2021
[2] Bogaerts, A.; Tu, X.; Whitehead, J. C.; Centi, G.; Lefferts, L.; Guaitella, O.; Azzolina-Jury, F.; Kim, H.-H.; Murphy, A. B.; Schneider, W. F.; Nozaki, T.; Hicks, J. C.; Rousseau, A.; Thevenet, F.; Khacef, A.; Carreon, M. J. Phys. Appl. Phys. 2020.
[3] Mehta, P.; Barboun, P. M.; Engelmann, Y.; Go, D. B.; Bogaerts, A.; Schneider, W. F.; Hicks, J. C. *ACS Catal.* **2020**
[4] Bayer, B. N.; Raskar, S.; Adamovich, I. V.; Bruggeman, P. J.; Bhan, A. *Plasma Sources Sci. Technol.* **2023**